vienna2006

A038

Full Waveform Tomography and Nonlinear Migration

W.A. Mulder* (Shell International Exploration & Production) & R.E. Plessix (Shell International Exploration & Production BV)

SUMMARY

The least-squares functional measures the difference between observed and modelled seismic data. Because it has a high computational cost and suffers from local minima, it has limited use for the inversion of model parameters. A good initial velocity model is required. Given such a model, the minimisation of the least-squares functional resembles nonlinear migration more than inversion.

Several authors observed that the model could be updated by diving waves, without the risk of ending up in a local minimum. They used frequency-domain acoustic modelling codes to construct a velocity model. This full waveform tomography is limited to a maximum depth, determined here by considering a simple model. This creates a dichotomy. Down to the maximum depth of diving waves, least-squares minimisation combines tomography and migration. Beyond that depth, nonlinear migration dominates. The dichotomy has consequences for the choice of frequencies when using a frequency-domain acoustic modelling code.

The acoustic approximation will lead to a number of problems when using long-offset data. We show that reasonable results can still be obtained on synthetic marine data created by an elastic time-domain finite-difference code. The resulting density is not correct, but the overall geometry is.

Introduction

Albert Tarantola [6] pioneered full waveform inversion in the 1980s with the aim to find a subsurface model that produced the best fit to seismic data. Attempts were only partially successful, because the least-squares misfit functional suffers from local minima. A good initial model is required to prevent gradient-based optimization methods from ending up in the wrong minimum. Later, it was realized that long-offset data could help to avoid the problem of local minima (see [4,5] and references therein). These data contain diving waves that allow for tomographic velocity inversion in parts of the subsurface traversed by these waves. A complementary approach was adopted in [2,3] with the focus on migration, assuming that the initial velocity model is sufficiently close to the global minimum. This nonlinear iterative migration method is algorithmically the same as full waveform tomography, with the distinction that the emphasis is on the determination of the short-wavelength structure of the subsurface model. Nevertheless, diving waves will also update the long-wavelength velocity components of the model.

Here will we address several issues in tomographic inversion and nonlinear migration that may arise when a frequency-domain acoustic modelling code is used. The depth of the computational domain is determined by the diving waves. The choice of frequencies will be different for tomography and for migration. The acoustic approximation may cause some problems. A synthetic marine example based on elastic modelling will serve as an illustration.

Diving waves

Diving waves can be related to turning rays in a smooth background velocity model. To obtain an estimate of the depth z_{max} that is reached by diving waves for an offset h, we assume that the velocity increases linearly with depth: $v(z) = v_0 + \gamma z$. Ray theory predicts $z_{max} = [(v_0/\gamma)^2 + (h/2)^2]^{½} - (v_0/\gamma)$. Figure 1 shows the maximum depth as a function of offset for a number of velocity gradients and $v_0 = 1.5$ km/s. Note that there is a significant increase in the maximum depth when going from 3 to 6 km. For very large offsets, z_{max} tends to ½h. Figure 2a shows the slowness gradient for a model with $v_0 = 800$ m/s and $\gamma = 0.7$ s^{-1} at 12 Hz and assuming zero synthetic data. The result for many sources is shown in Fig. 2b, obtained by stacking of Fig. 2a in the horizontal direction. The strongest peaks lie around to $z_{max} = 2.1$ km. An estimate of the width of the peak is given by the size of the Fresnel zone at maximum depth. This size is of the order of $w_F = (\lambda L/8)^{½}$, where L is the total distance travelled by the ray from source to receiver and λ the wavelength. If we adopt $v(z_{max})/f$ for the latter, we find a width $w_F = 0.43$ km. The result at depths beyond about z_{max} is useless for tomography. If we take offsets between 100 m and 6 km at 25 m spacing, we obtain the summed result shown in Fig. 3. Since the modelled data were set to zero, the gradient wants to remove the linear velocity profile. The result is only useful down to the value of $z_{max} - w_F$ for 6 km offset. In practice, the maximum depth for tomography will range from a quarter to a third of the maximum offset for present-day long-offset data sets.

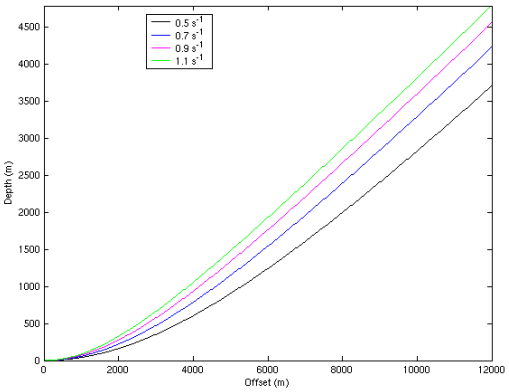

Figure 1: Maximum depth reached by turning rays as a function of offset, for various choices of the velocity gradient.

Choice of frequencies

The choice of frequencies is different for nonlinear migration and tomography. For migration, aliasing in depth is avoided by requiring a frequency spacing not exceeding $\Delta f = ½v/[\{z^2 + (h/2)^2\}^{½} - (h/2)]$ where v is the effective velocity up to depth z [2]. For tomography, the choice can be based on continuous vertical wave number coverage [5]. The frequencies obey $f_{n+1} = f_n/\alpha$, where $\alpha = z/\{z^2 + (h/2)^2\}^{½} < 1$, starting from a smallest frequency f_0. Here h is the

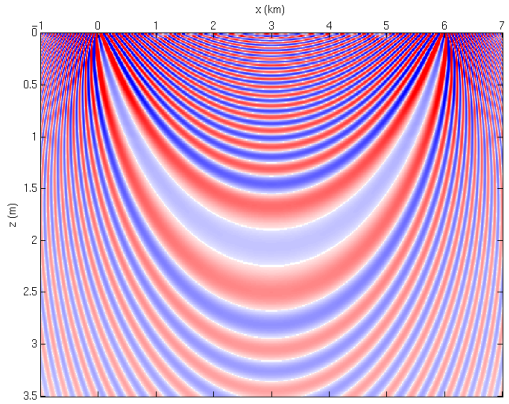

Figure 2a: Slowness gradient at 12 Hz for a source at the origin and a receiver at 6 km.

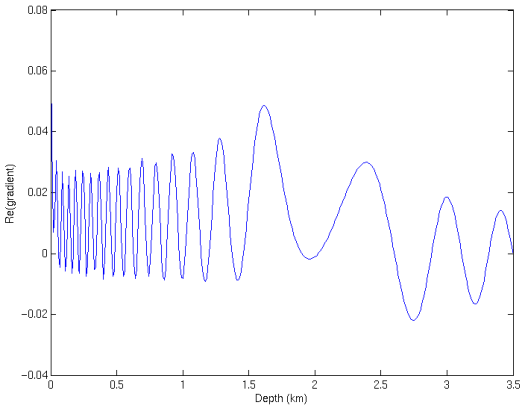

Figure 2b: Horizontal stack of Fig. 2a. The result is useless beyond the first large peak.

maximum offset and z the depth of the target. A complementary approach might be based on the observation that diving waves already provide a good velocity update for a single frequency. Therefore, avoiding local minima should motivate the choice of frequencies for tomography. The first frequency should be the lowest in the data, and higher frequencies should fill in the details of the model. For computational reasons, the number of frequencies should be kept small. The choice of the next higher frequency should then be determined by the requirement that we stay just within the basin of the global minimum. We expect that the size of the basin will decrease with increasing frequency. Presently, it is not clear if this leads to the same criterion as in [5].

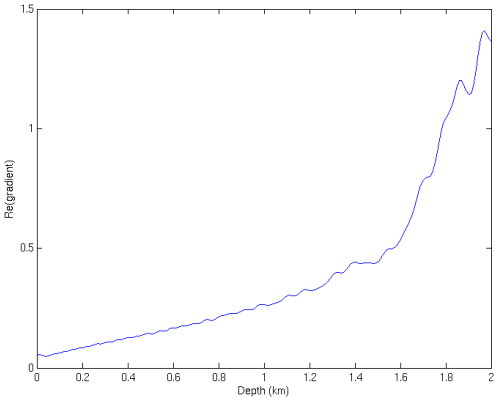

Figure 3: Reciprocal of the velocity gradient after stacking all offsets.

Problems with real data

Real data are more accurately described by an elastic than an acoustic model. If we insist on using an acoustic 2D code for cost and complexity reasons, we will run into a number of problems. Firstly, let us assume that we are dealing with marine data and that the sea water velocity model and sea bottom position are known. The long offset data related to the sea bottom reflections will then display a phase difference when comparing acoustic to elastic reflections/refractions. An obvious remedy is the use of a smooth velocity model to first process the diving waves and then fill in the sea bottom and layering by introducing the shorter offsets. Secondly, the effective velocity seen by a refracted wave in an elastic medium can be different from the P-velocity. If we only have sediments with small contrasts, events will consists of diving waves and pre-critical reflections. Acoustics should then suffice. Strong contrasts, such as salt bodies or basalt layers, will generate post-critical events that may lead to the wrong velocity below the top of the salt or basalt. Thirdly, thin-bed layering of sediments will result in an effective anisotropy. If that is ignored, the velocities produced by tomography of diving waves will represent the effective horizontal rather than the vertical velocity. Fourthly, converted waves and 3D effects may cause unwanted effects.

Synthetic example

To study some of these effects, we generated 5 seconds of data with a time-domain elastic finite-difference code for the Marmousi2 model [1] with shots in the range between 12 and 5 km at a 50 m interval and 7.5 m depth. The receivers had offsets between 200 and 6000 m to

the right side of the shot at a 25 m interval and the same depth. A free-surface boundary condition was included. The P-velocity and density, but not the S-velocity, are shown in Figure 4. Frequencies were chosen to avoid depth aliasing in nonlinear migration [2] and ranged from 6 to 15 Hz at a 0.2 Hz interval. Because the original wavelet was not zero-phase, it was estimated by fitting the direct wave for one shot. The result was used to change the phase of the data as if they had been generated by a zero-phase wavelet. The modified wavelet peaked at 12 Hz. Next, a shallow model was constructed for the sea bottom and the sediments just below. This was spliced into a very smooth velocity model obtained by adjoint interpolation onto a spline grid with 400 m spacing, which was then interpolated back to a 10 m grid. The initial density was based on Gardner's rule.

The maximum depth reached by diving waves can be found by inspection. Figure 5 shows the gradient with respect to slowness in the initial model, on the left for all the frequencies, on the right for a single frequency and both for all shots and receivers. In spite of the presence of reflectors and guided waves, one might discern diving waves down to about 2.5 km depth. Both waveform tomography and nonlinear migration will play a role down to that depth. Beyond, the model updates will be dominated by reflections and we are operating in "migration mode". This implies that we should work with the frequencies that avoid aliasing. The result after hundreds of iterations is shown in Figs 6 and 7. The rough part of the impedance obtained by applying a spatial high-pass filter is displayed in Fig. 6. It resembles a typical migration image. The exact result is shown for comparison. Figure 7 shows the velocity and density. The density differs from the true density as it tries to mimic elastic effects in an acoustic model. The least-squares functional has reached a value of 0.21 times the data energy, which may seem quite large but is considerably smaller than usually found for real marine data sets.

Conclusions

We have discussed a number of issues and problems in acoustic full waveform tomography and nonlinear migration when using a frequency domain code. Tomographic inversion based on diving waves can be used down to a depth that can be estimated by assuming a simple linear velocity model with depth or by inspection of the gradient for a single frequency in a more realistic model. The computational domain should be limited to that depth if tomography with one or a few frequencies is the goal. Beyond, we are in migration mode and sufficiently many frequencies should be used to avoid aliasing in depth. Elastic effects and effective anisotropy may limit the validity of long-offset tomographic inversion.

References

[1] Martin, G., 2004. The Marmousi2 Model, Elastic Synthetic Data, and an Analysis of Imaging and AVO in a Structurally Complex Environment, PhD Thesis, University of Houston, Texas, USA (http://www.agl.uh.edu/).

[2] Mulder, W.A., and Plessix, R.-E., 2004. How to choose a subset of frequencies in frequency-domain finite-difference migration, Geophysical Journal Int.158, 801–812.

[3] Mulder, W.A., and Plessix, R.-E., 2004. A comparison between one-way and two-way wave-equation migration, Geophysics 69, 1491–1504.

[4] Ravaut, C., Operto, S., Improta, L., Virieux, J., Herrero, A., and Dell'Aversana, P., 2004. Multiscale imaging of complex structures from multifold wide-aperture seismic data by frequency-domain full-waveform tomography: application to a thrust belt, Geophysical Journal International 159, 1032–1056.

[5] Sirgue, L., and Pratt, R.G., 2004. Efficient waveform inversion and imaging: A strategy for selecting temporal frequencies, Geophysics 69, 231–248.

[6] Tarantola, A., 1984. Inversion of seismic reflection data in the acoustic approximation. Geophysics 49, 1259–1266.

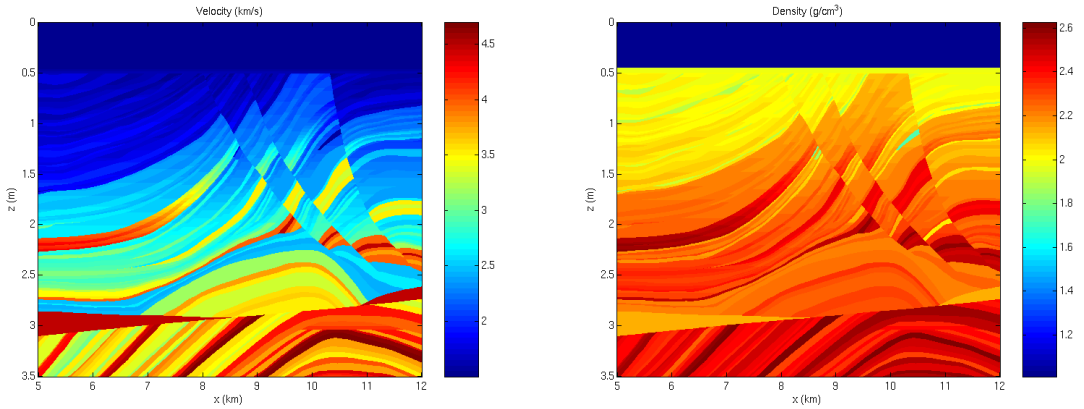

Figure 4: The original velocity (left) and density (right) model.

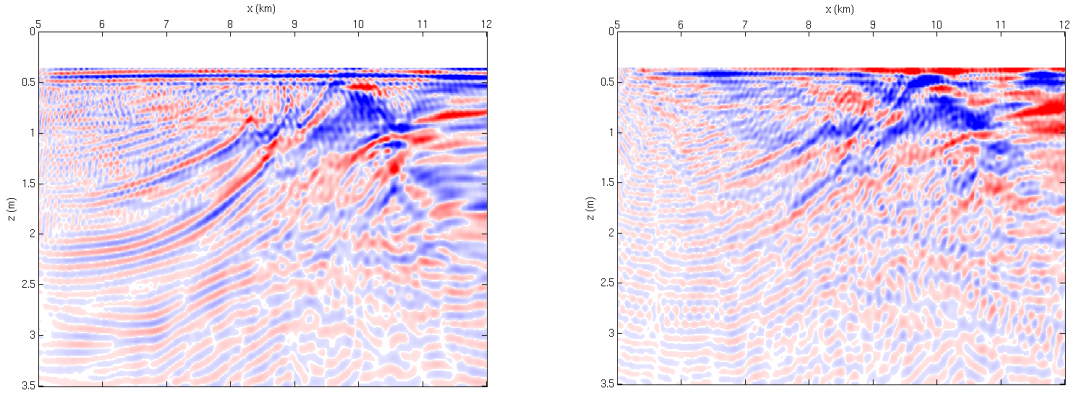

Figure 5: Slowness gradient, clipped at 50%, obtained with the unaliased frequencies (left) and 12 Hz only (right). Diving waves are visible down to about 2.5 km depth in both cases.

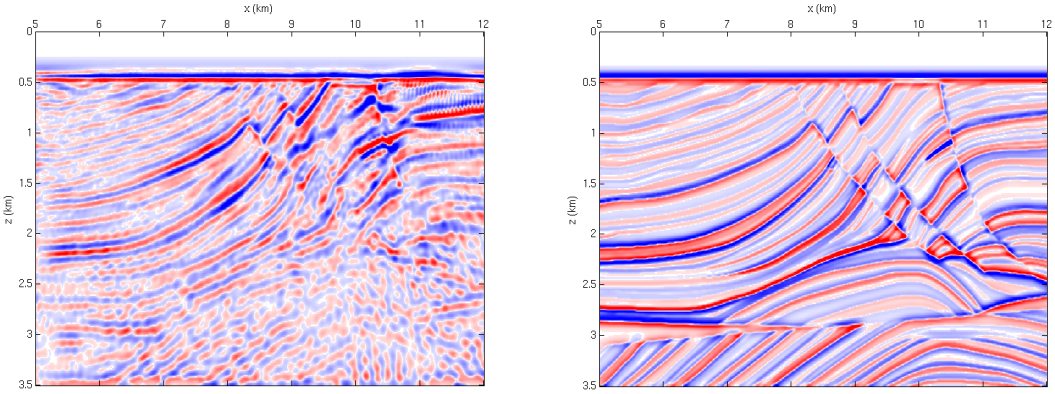

Figure 6: The rough part of the impedance obtained with the unaliased frequencies is shown on the left, the exact answer on the right.

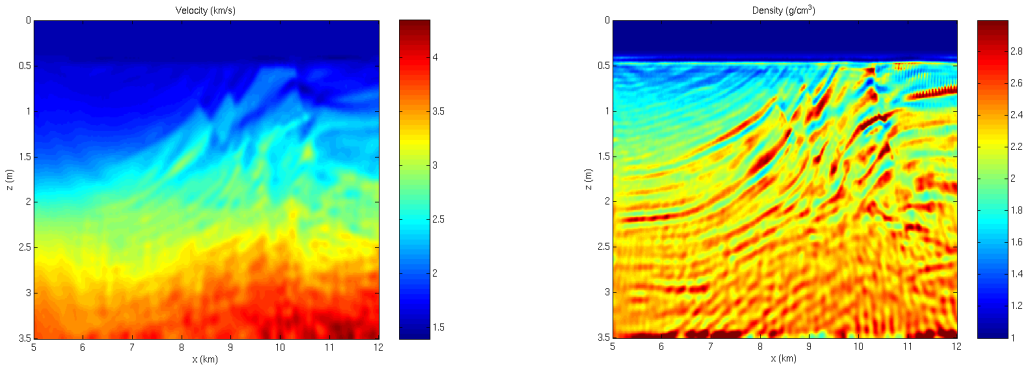

Figure 7: Velocity (left) and density (right) obtained after hundreds of iterations, using unaliased frequencies.